



Obrabotka metallov - Metal Working and Material Science

Journal homepage: http://journals.nstu.ru/obrabotka_metallov



Investigation of the structural-phase state and mechanical properties of ZrCrN coatings obtained by plasma-assisted vacuum arc evaporation

Andrey Filippov^{1, a,*}, Nikolay Shamarin^{1, b}, Evgenij Moskvichev^{1, c}, Ol'ga Novitskaya^{1, d},
 Evgenii Knyazhev^{1, e}, Yuliya Denisova^{2, f}, Andrei Leonov^{2, g}, Vladimir Denisov^{2, h}

¹ Institute of Strength Physics and Materials Sciences SB RAS, 2/4, pr. Akademicheskii, Tomsk, 634055, Russian Federation

² Institute of High Current Electronics SB RAS, 2/3 Akademicheskoy Avenue, Tomsk, 634055, Russian Federation

^a  <https://orcid.org/0000-0003-0487-8382>,  andrey.v.filippov@yandex.ru, ^b  <https://orcid.org/0000-0002-4649-6465>,  shnn@ispms.ru,

^c  <https://orcid.org/0000-0002-9139-0846>,  em_tsu@mail.ru, ^d  <https://orcid.org/0000-0003-1043-4489>,  nos@ispms.tsc.ru,

^e  <https://orcid.org/0000-0002-1984-9720>,  zhenya4825@gmail.com, ^f  <https://orcid.org/0000-0002-3069-1434>,  yukolubaeva@mail.ru,

^g  <https://orcid.org/0000-0001-6645-3879>,  laa-91@yandex.ru, ^h  <https://orcid.org/0000-0002-5446-2337>,  volodyadenisov@yandex.ru

ARTICLE INFO

Article history:

Received: 10 December 2021

Revised: 28 December 2021

Accepted: 28 January 2022

Available online: 15 March 2022

Keywords:

Coating

Morphology

Nitrides

Structure

Phase composition

Funding

The work was carried out with financial support from the Russian Federation represented by Ministry of Science and Higher Education (Project No. 075-15-2021-1348) within the framework of event No. 1.1.16.

Acknowledgements

Research were partially conducted at core facility "Structure, mechanical and physical properties of materials"

ABSTRACT

Introduction. Modern technologies allow the synthesis of nanostructured coatings from multiple chemical elements to combine different physical, mechanical, and chemical properties in one coating. Promising in this respect are coatings formed via layer-by-layer deposition of zirconium and chromium nitrides. The deposition of various chemical elements on various substrates requires separate studies in order to produce high-strength and wear-resistant coatings. **The purpose of this work** is to study the structural-phase state and mechanical properties of ZrCrN coatings formed by plasma-assisted vacuum arc evaporation. **Materials and methods.** The investigation is performed on specimens comprising VK8 hard alloy substrates with zirconium and chromium nitride coatings as well as with multilayer ZrCrN coatings. The methods used are confocal laser scanning microscopy, X-ray diffraction analysis, high-resolution scanning electron microscopy, nanoindentation, and scratching. **Results and discussion.** The experimental results obtained showed that the mode of multilayer ZrCrN coating evaporation greatly affects the structure, morphology, surface roughness, and mechanical properties of the coatings. In particular, by varying the substrate rotation speed during coating deposition it is possible to control the deposition time of each coating layer and thereby modify the layer properties. **Conclusions.** The investigation results showed that variation of the evaporation conditions allows one to obtain a ZrCrN coating with a high nanohardness of 45 GPa on a VK8 alloy substrate. Analysis of mechanical test results indicate good adhesion between the studied coatings and the substrate. Scratch tests revealed that fracture of CrN and ZrN coatings occurs by the cohesive mechanism, and the surface of ZrCrN coatings exhibits uniform scratches without any signs of fracture. Based on the results obtained, ZrCrN-2...ZrCrN-4 coatings can be recommended for use as hard and wear-resistant coatings.

For citation: Filippov A.V., Shamarin N.N., Moskvichev E.N., Novitskaya O.S., Knyazhev E.O., Denisova Yu.A., Leonov A.A., Denisov V.V. Investigation of the structural-phase state and mechanical properties of ZrCrN coatings obtained by plasma-assisted vacuum arc evaporation. *Obrabotka metallov (tehnologiya, oborudovanie, instrumenty) = Metal Working and Material Science*, 2022, vol. 24, no. 1, pp. 87–102. DOI: 10.17212/1994-6309-2022-24.1-87-102. (In Russian).

* Corresponding author

Filippov Andrey V., Ph.D. (Engineering), Senior Researcher
 Institute of Strength Physics and Materials Sciences SB RAS
 2/4, pr. Akademicheskii,
 634055, Tomsk, Russian Federation
 Tel.: 8 (999) 178-13-40, e-mail: andrey.v.filippov@yandex.ru

Introduction

One of the methods for improving the performance of parts and components is to cover its elements with coatings that have higher physical, mechanical, and chemical properties than the base metal. A rational choice of the coating composition, deposition technique and conditions will determine the properties of the coatings and characteristics of the improved products.

Modern technologies allow synthesizing coatings from multiple chemical elements in order to combine its different physical, mechanical and chemical properties in one coating. This is most often done through the formation of multilayer coatings with thin nanostructured layers [1]. The alternating layers provide an effective combination of various functional properties such as wear resistance, corrosion resistance, high hardness, etc. in one coating. Therefore, the choice of the composition of each layer will determine the resulting performance characteristics of the product.

The most effective approach to the formation of multilayer coatings implies the deposition of one layer with high hardness and the other with the ability to absorb strain energy. This combination gives a coating with high hardness but not prone to brittle fracture at large strains, which is a desired goal of modern technology [2]. An important aspect is that modern types of equipment operate in high-power modes with high operating temperatures at which coatings must retain its properties. Thus, the high temperature resistance is also a necessary coating property in addition to the already mentioned ones.

Chromium and zirconium nitride coatings correspond in some respects to the above requirements. It is known that ZrN coatings have high wear resistance and can effectively absorb mechanical strain energy during friction [3–8]. A single-layer CrN coating has low wear resistance due to columnar structure [9–12], while a multilayer coating of the same material has a much higher wear resistance [13–17], indicating a high structural sensitivity of the given material. Both of these types of coatings have high thermal stability and chemical resistance [14, 18]. Therefore, by alternating ZrN and CrN layers it is possible to obtain $ZrCrN$ coatings with high physical and mechanical properties.

Multilayer $ZrCrN$ coatings can be applied by various methods [19]. The most widely known *PVD* techniques are magnetron sputtering [20–25] and vacuum arc evaporation [26–30]. The latter method provides high adhesion between the coating and the substrate, and allows flexible control over the composition and thickness of the deposited layer due to a wide-range variation of the energy of condensed ions.

The literature reviews in [29, 30] indicate that the hardness of multilayer $ZrCrN$ coatings deposited on TiC substrates strongly depends on its deposition conditions and, as a rule, does not exceed 30 GPa. A higher hardness (up to 42 GPa) was achieved in nanostructured multilayer $ZrCrN$ coatings deposited on corrosion-resistant steel $12Cr18Ni10Ti$ [27]. Consequently, the substrate strongly affects the final application properties of the coating. As far as we know there are no reports on multilayer $ZrCrN$ coatings deposited on $VK8$ alloy, which is widely used for industrial metal forming and cutting tools.

The purpose of this work is to study the structural-phase state and mechanical properties of $ZrCrN$ coatings deposited by plasma-assisted vacuum arc evaporation on $VK8$ alloy substrates.

Research methods

Coatings were deposited by vacuum arc plasma evaporation. In the experiment, metal plasma was generated using two electric arc evaporators with 80-mm-diameter cylindrical cathodes made of $E110$ Zr alloy and 99.9% purity Cr . Gas plasma was generated by a plasma source with a thermionic and hollow cathode. The gas plasma source was used for cleaning, heating and chemical activation of the sample surfaces by gas ion bombardment, as well as for additional gas ionization and plasma-assisted coating deposition. $VK8$ hard alloy samples with a diameter of 10 mm and a thickness of 7 mm were mounted on a rotating planetary substrate holder at a distance of about 20 cm from the chamber axis at the exits of the plasma sources.

Before the start of the experiment, the vacuum chamber with dimensions of about $650 \times 650 \times 650$ mm³ was evacuated to a limiting pressure of 10^{-2} Pa using a *TMP1000* turbomolecular pump. Argon plasma gas

was introduced through the plasma source to a working pressure of 0.3 Pa. By triggering a gas discharge with a current of about 40 A and applying a bias voltage of 700 V to the substrate holder with the hard alloy samples, the substrates were heated to a temperature of 400 °C. After ion bombardment cleaning of the sample surfaces and its chemical activation, a nitrogen-argon mixture in a percentage ratio of 90/10 (N₂:Ar) was injected to a pressure of 0.5 Pa and arc discharges with currents of 80 A were triggered in the evaporators.

Along with multilayer *ZrCrN* coatings, *ZrN* and *CrN* coatings deposited under similar conditions, but using only one of the cathodes, were examined for a comparative analysis of the coating properties. The phase composition and properties of multilayer coatings were changed by varying the rotation speed of the sample holder. Four holder rotation speeds were used: 0.5 rpm (designation for *ZrCrN-1* sample), 3.5 rpm (*ZrCrN-2*), 5 rpm (*ZrCrN-3*), and 8 rpm (*ZrCrN-4*). The holder rotation speed during the deposition of *ZrN* and *CrN* coatings was 0.5 rpm.

Nanoindentation was performed on a *NHT-TTX S* nanoindentation tester (CSEM, Switzerland) with a linearly increasing load from 0 to 25 mN and a loading rate of 1.5 μm/min. The nanoindentation data were analyzed by the *Oliver–Pharr* method.

Scratch indentation was performed on a *Revetest RST* macro scratch tester (CSM Instruments, USA) with a Rockwell diamond indenter, a scratching speed of 3 mm/min, a scratch length of 3 mm, and a linearly increasing load from 0 to 50 N.

X-ray diffraction analysis was performed using a *DRON-7* X-ray diffractometer (Burevestnik, Russia) in the angle range $2\Theta = (20-90)^\circ$ and with the X-ray wavelength $\lambda = 1.54 \text{ \AA}$.

The surface morphology of the samples was examined using an *Apreo 2 S* high-resolution scanning electron microscope (FEG SEM) (Thermo Fisher Scientific, USA). The cross section of the coatings was examined on fracture surfaces.

The surface roughness was examined using an *Olympus OLS LEXT 4100* confocal laser scanning microscope (Olympus, Japan).

Results and discussion

The surface images of the studied coatings are presented in Figure 1. One can see small black dots on the surface of all samples. Surface examination by confocal laser scanning microscopy revealed that these points are both droplet inclusions on the surface and pores. It appears visually similar and has comparable diameters of the order of 0.5–5 μm. The number and size of these dots are larger on the surface of multilayer *ZrCrN* coatings (Figs. 1c–1f) compared with *ZrN* (Fig. 1a) and *CrN* (Fig. 1b) coatings.

Surface roughness analysis was performed with the *Olympus LEXT* software to quantify differences in the surface morphology of the coatings. The evaluation was carried out using two parameters *Sa* and *Sz*, which are the arithmetic mean and the maximum height of surface microroughness, respectively. The analysis data (Fig. 2) indicate that the roughness of multilayer *ZrCrN* coatings in terms of the *Sa* parameter is by a factor of 1.8–2.9 higher compared to *CrN* coating, and a factor of 1.1–1.8 than for *ZrN* coating. A much less increase in the roughness of multilayer *ZrCrN* coatings is observed in terms of the *Sz* parameter, which is by a factor of 1.5–1.8 higher compared to *CrN* and only 3–15 % higher compared to *ZrN*. It follows from the data obtained that surface roughness in terms of the *Sa* parameter increases monotonically from the sample with *CrN* coating to the sample with multilayer *ZrCrN-4* coating. Increasing the substrate holder rotation speed from 0.5 to 8 rpm leads to an ~38% increase in surface roughness in terms of the *Sa* parameter. The surface roughness change due to variation in the deposition conditions for samples with multilayer *ZrCrN-1...ZrCrN-4* coatings in terms of the *Sz* parameter is less significant and does not exceed 12 %.

Surface roughness measurements of the coatings by confocal laser scanning microscopy allow evaluating such parameters as the roughness amplitude and the number of roughness elements per unit area. This is done according to GOST R ISO 25178-2-2014 that involves the determination of the void volume, peak volume, and core material volume.

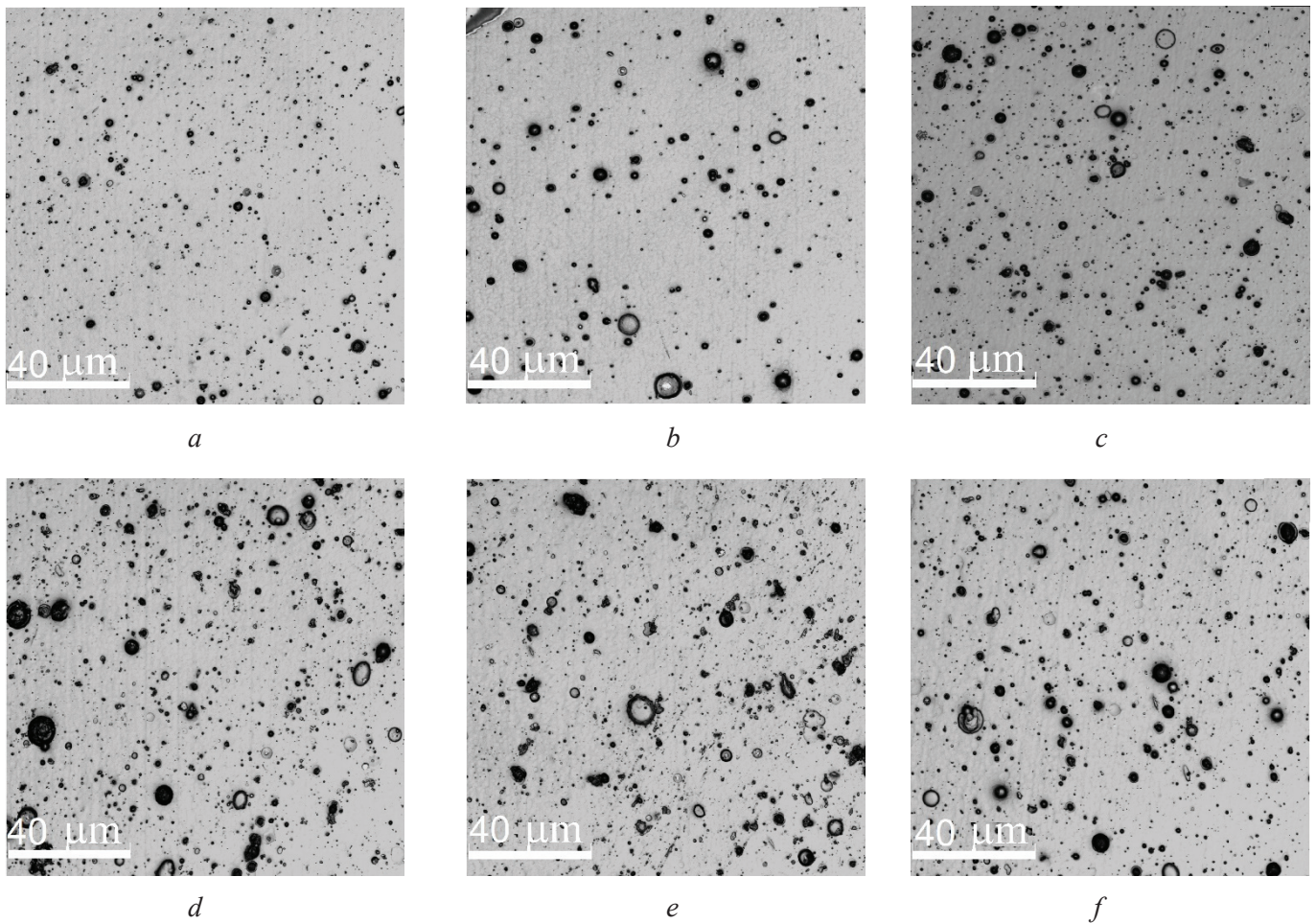


Fig. 1. Surface images of samples coated with: *CrN* (a), *ZrN* (b), *ZrCrN-1* (c), *ZrCrN-2* (d), *ZrCrN-3* (e), *ZrCrN-4* (f)

ZrCrN coatings demonstrate a significant increase in the total void volume (V_{vv} increases by a factor of 2.25–3.75 compared with *CrN* coating and 1.13–1.88 compared with *ZrN*) and the core void volume (V_{vc} increases by a factor of 1.34–1.49 compared with *CrN* coating and 1.12–1.24 compared with *ZrN*).

The peak and core material volumes also increase greatly for *ZrCrN* coatings (V_{mp} increases by a factor of 2.88–5.25 compared with *CrN* coating and 1.77–3.23 compared with *ZrN*; V_{mc} increases by a factor of 1.31–1.38 compared with *CrN* coating and 1.21–1.29 compared with *ZrN*).

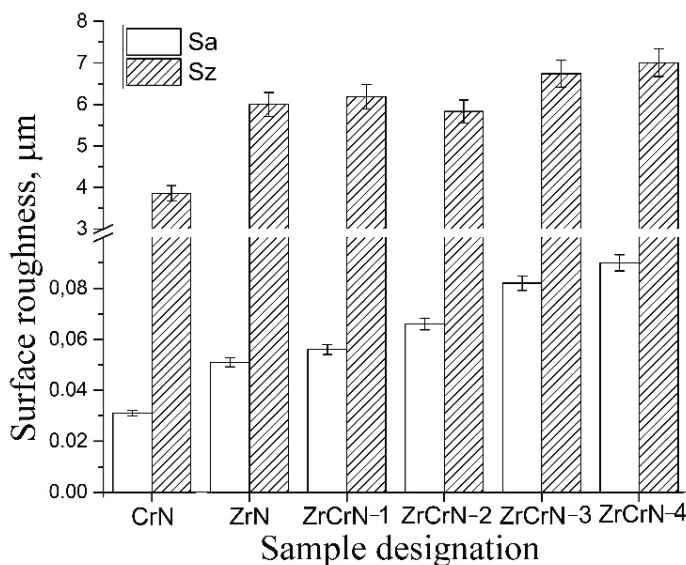


Fig. 2. Surface roughness of coatings

The increase in the total void volume (V_{vv}) and peak material volume (V_{mp}) indicates that *ZrCrN* coatings contain a larger number of peaks and valleys per unit area compared with *CrN* and *ZrN* coatings. This quantitatively agrees with the roughness measurement results. However, the obtained estimates show that the peak material volumes exceed the total void volumes. As for the core, it is obvious that the core void volume (V_{vc}) exceeds the core material volume (V_{mc}).

The coating surfaces were also examined by high-resolution scanning electron microscopy. It can be seen that the morphology of *CrN* (Fig. 4a) and *ZrN* (Fig. 4b) coatings differs significantly. *CrN* coating has a nanocrystalline structure. *ZrN*

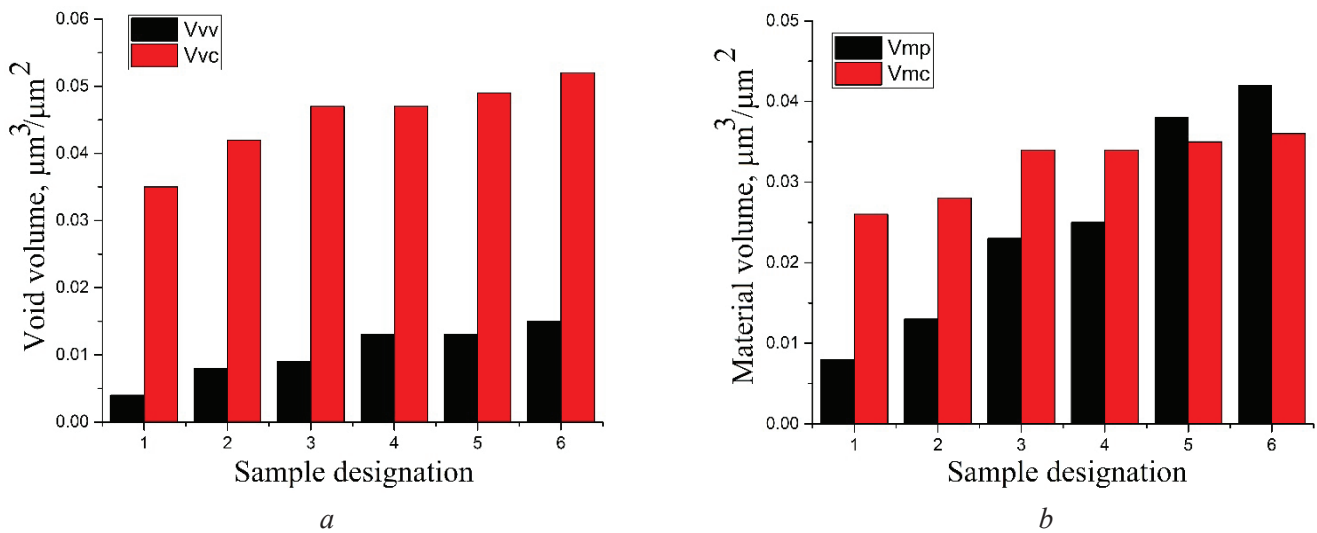


Fig. 3. Void volume (a) and material volume (b) per unit area of coatings: CrN (1), ZrN (2), ZrCrN-1 (3), ZrCrN-2 (4), ZrCrN-3 (5), ZrCrN-4 (6)

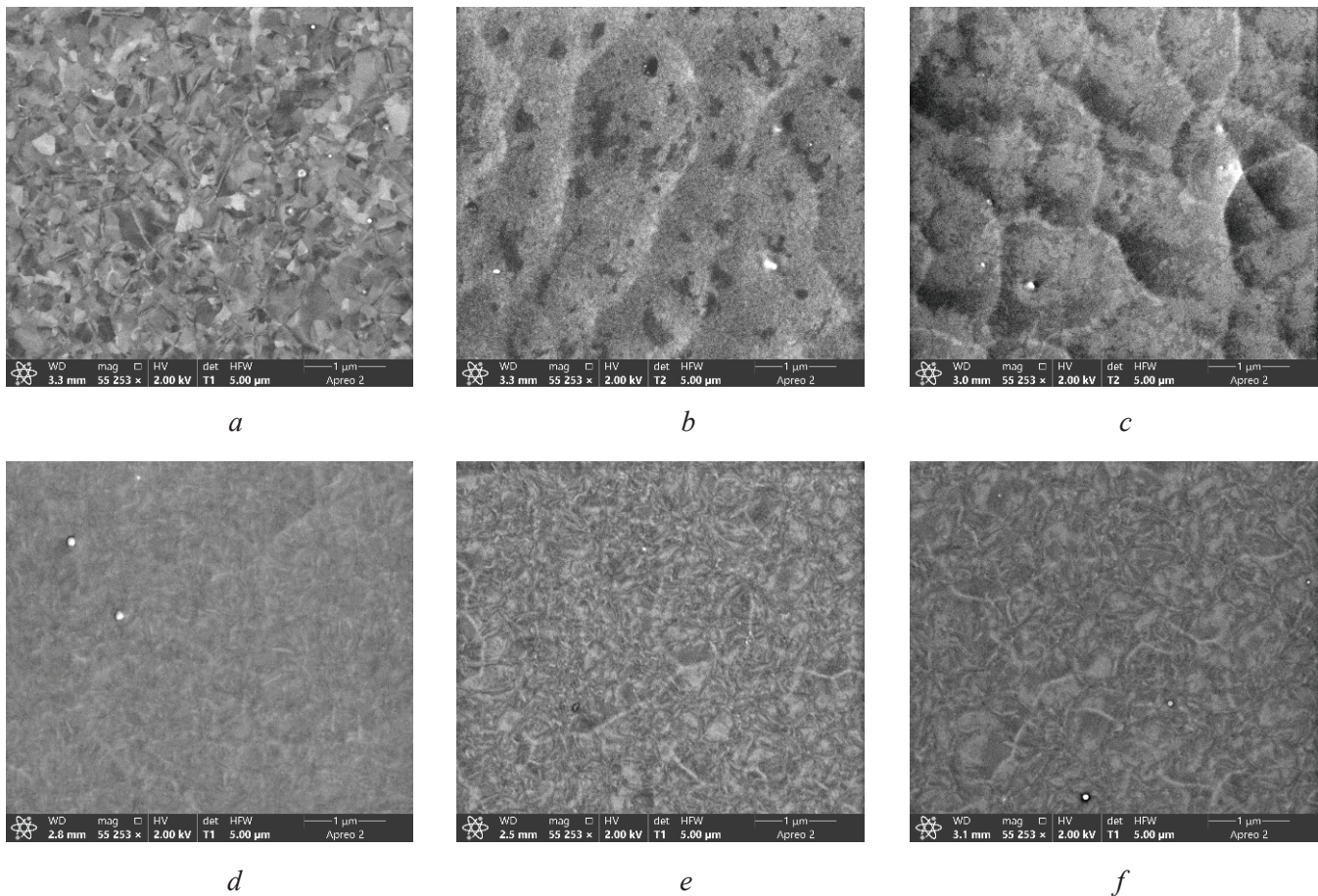


Fig. 4. SEM images of the coating surface: CrN (a), ZrN (b), ZrCrN-1 (c), ZrCrN-2 (d), ZrCrN-3 (e), ZrCrN-4 (f)

coating exhibits no grains and has an inhomogeneous surface relief, which is consistent with the roughness studies. Multilayer ZrCrN-1 coating (Fig. 4c) is similar in surface morphology to ZrN, as its upper layer is of zirconium nitride. The surface morphology of ZrCrN-2...ZrCrN-4 coatings is represented by smaller elements, but it is difficult to classify it into independent elements due to its nanoscale size.

The cross-sectional image of the fracture surface of *ZrCrN-1* coating (Fig. 5a) shows its multilayer structure with an average layer thickness of ~ 100 nm. The planarity of the layers is slightly distorted; no defects such as pores or delaminations are observed; the interface with the substrate is also free of defects. The total number of layers in the coating is 72.

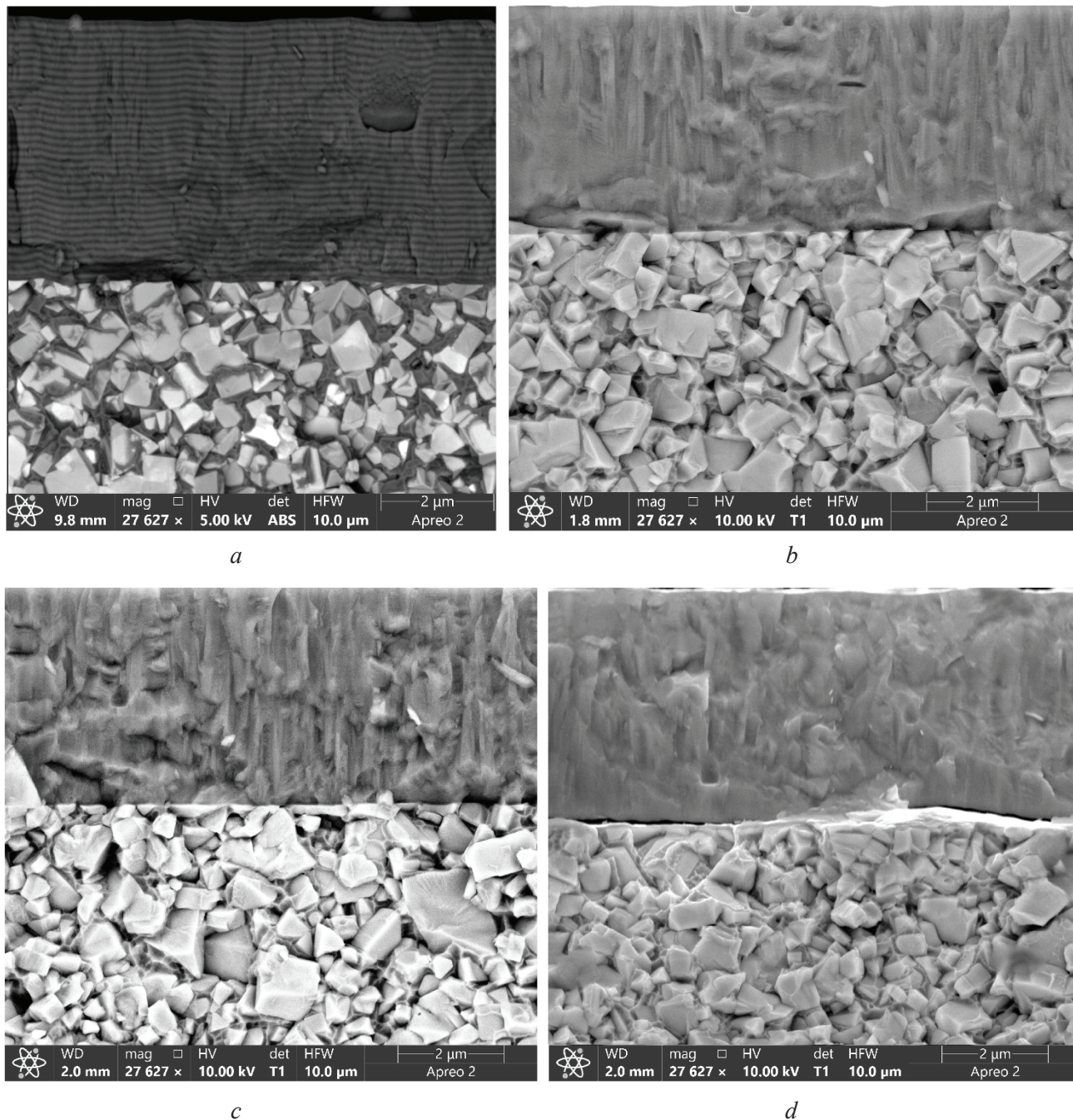


Fig. 5. Cross-sectional SEM images of the fracture surface of multilayer coatings: *ZrCrN-1* (a), *ZrCrN-2* (b), *ZrCrN-3* (c), *ZrCrN-4* (d)

The SEM micrograph of the fracture surface of *ZrCrN-2*...*ZrCrN-4* coatings (Figs. 5b–5d) also exhibits a nanosized structure, but without well-defined layers. The thickness of *ZrCrN* coatings is about 4.5 ± 0.5 μm. The absence of significant defects at the substrate–coating interface indicates a strong bond and good adhesion between the coating and the substrate. Otherwise, the coating would locally peel off as a result of cleavage.

Analysis of X-ray diffraction profiles (Fig. 6) showed that the X-ray intensity is rather high and radiation reaches not only the coating but also the substrate, as confirmed by the presence of reflections belonging

to the *WC* phase. *CrN* and *ZrN* coatings have a pronounced (111) texture, which follows from the magnitude of the reflections in the diffraction profiles and the almost complete absence of other phase reflections for these coatings. Multilayer *ZrCrN* coatings have reflections of both zirconium nitride and chromium nitride, but *ZrN* are more intense. The *ZrN*(220) reflection is quite broad for *ZrCrN*-2...*ZrCrN*-4 samples. The *ZrN*(111) reflection is shifted and its intensity is lower. These changes in the diffraction profiles may indicate the nanostructured state of the coating in these samples. The phase composition of *ZrCrN*-4 coating cannot be effectively assessed as, in addition to the above, there is a significant shift and superposition of many reflections.

The mechanical properties of the coatings were studied by nanoindentation and scratching. Typical loading curves during nanoindentation are shown in Figure 7. The load was selected in such a way that the indentation depth was less than the coating thickness. At the first glance, the plotted curves clearly demonstrate that the mechanical properties of the studied coatings are different. The values of nanohardness and reduced elastic modulus were obtained after data processing by the *Oliver–Farr* method using specialized software

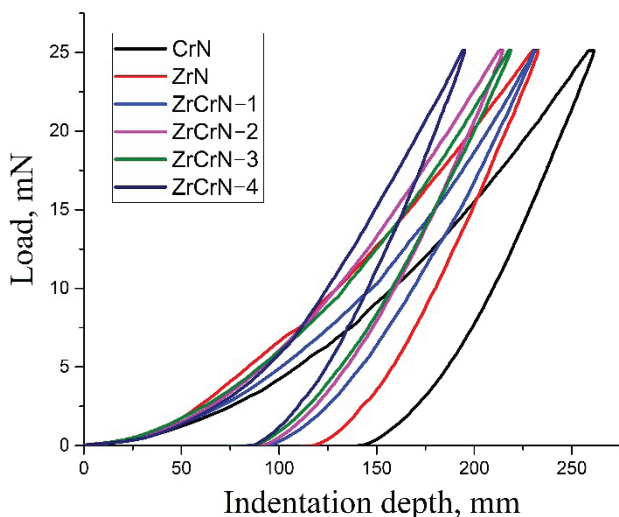


Fig. 7. Nanoindentation loading curves of coatings

here, but, as in [26], the peaks of the *ZrN* and *CrN* reflections were shifted. This indicates a microdistortion of the crystal lattice, which may be the cause of changes in the mechanical properties of the material. For the case considered in this work, reflections in XRD profiles taken from *ZrCrN* coatings are also shifted (Fig. 6). It may also indicate lattice distortion that contributes to hardness enhancement. Similar results of the influence of lattice microdistortions on material hardness were earlier observed for austenitic steel produced by electron beam additive manufacturing [32].

The nanoindentation data are in qualitative agreement with the scratch test results. Figure 8 shows CLSM images of scratches on the surface of coatings. The first thing to note is that *CrN* (Fig. 8a) and *ZrN*

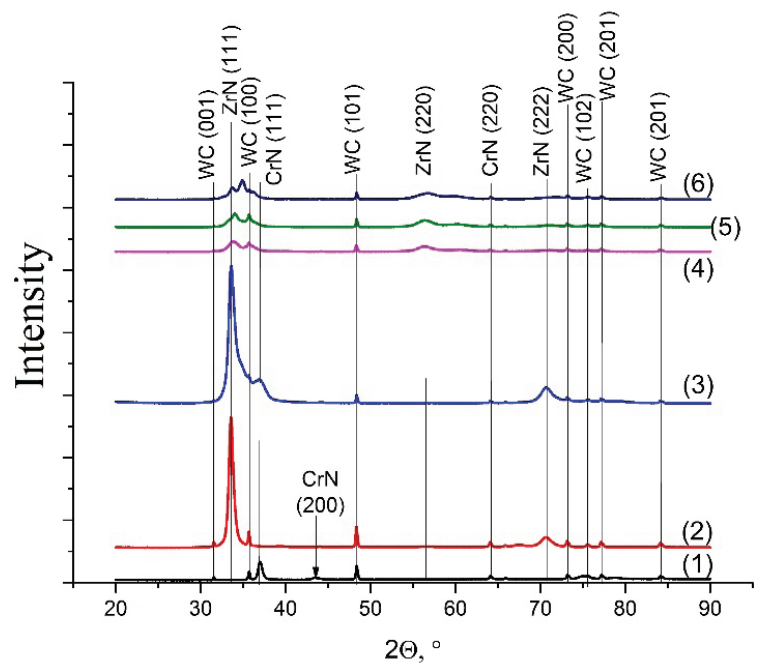


Fig. 6. X-ray diffraction profiles of coatings: *CrN* (1), *ZrN* (2), *ZrCrN*-1 (3), *ZrCrN*-2 (4), *ZrCrN*-3 (5), *ZrCrN*-4 (6)

(Table 1). The *H/E* ratio is often used as a measure of the coating resistance to elastic deformation, with an *H/E* greater than or equal to 0.1 being considered to indicate high quality of the coating [31]. It follows from the data that only three multilayer coatings meet this characteristic; the chromium nitride coating has the worst properties. The quality of the zirconium nitride coating can also be considered insufficient in terms of *H/E*.

It was shown in [26] that a decrease in the thickness of individual layers of multilayer *ZrN/CrN* coating from 300 to 20 nm allows increasing the hardness of the coating deposited on a *12Cr18Ni10Ti* steel substrate from 33 to 42 GPa. The decrease in hardness is also attributed in [26] to the formation of solid solutions of (*Zr;Cr*)*N* and (*Cr;Zr*)*N* near the (200) reflection. Such changes in the phase composition were not observed

Table 1

Nanoindentation test results

Sample	Nanohardness (H), GPa	Reduced modulus of elasticity (E), GPa	H/E
<i>CrN</i>	21.6	335	0.06
<i>ZrN</i>	29.8	394	0.08
<i>ZrCrN-1</i>	34	364	0.09
<i>ZrCrN-2</i>	37.5	359	0.1
<i>ZrCrN-3</i>	39.3	382	0.1
<i>ZrCrN-4</i>	45	436	0.1

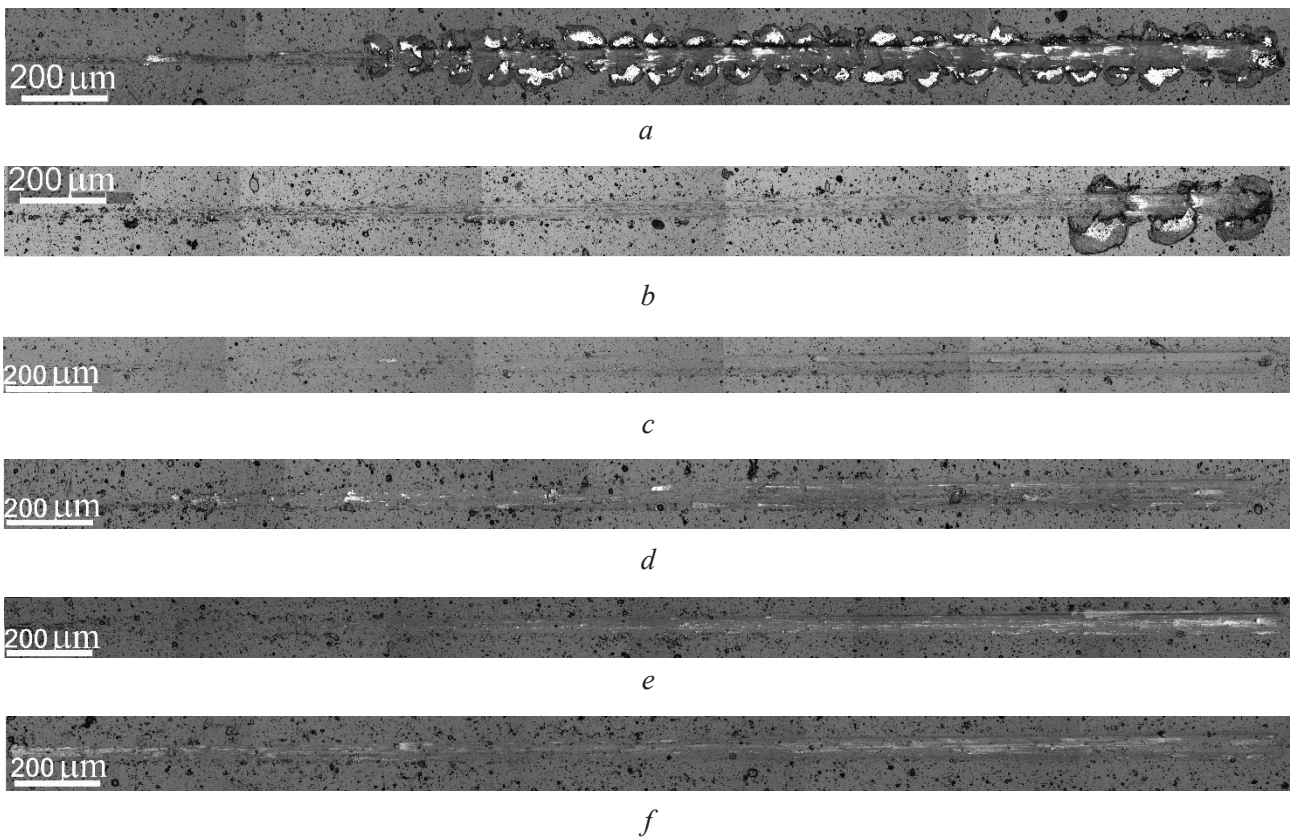


Fig. 8. Images of scratches on the surface of coatings: *CrN* (a), *ZrN* (b), *ZrCrN-1* (c), *ZrCrN-2* (d), *ZrCrN-3* (e), *ZrCrN-4* (f)

coatings (Fig. 8a) were scratched with a linearly increasing load. Multilayer *ZrCrN* coatings exhibit rather uniform scratches without cracks and cleavage. For a more detailed analysis of the effect of indentation on the coatings, the scratch profiles in the region of the deepest pit using the microscope software were evaluated (Fig. 9). The depth of scratches near the cleavage (Table 2) shows that the fracture of *CrN* and *ZrN* coatings is cohesive, because the depth of pits is smaller than the thickness of these coatings. The *CrN* coating fracture begins at a normal indentation load of ~ 12 N and that of *ZrN* begins at ~ 45 N. The tangential force was ~ 0.8 N for *CrN* coating and ~ 2.3 N for *ZrN*.

The change in the indentation depth during testing depends both on the coating properties and on the specified load. The load was set to increase linearly. Therefore, in the ideal case, the penetration of the indenter into the coating should occur in the same manner. However, this quantity slightly fluctuates in Fig. 10 (scratch length interval from 0 to ~ 2.3 mm), which is probably due to inhomogeneous surface

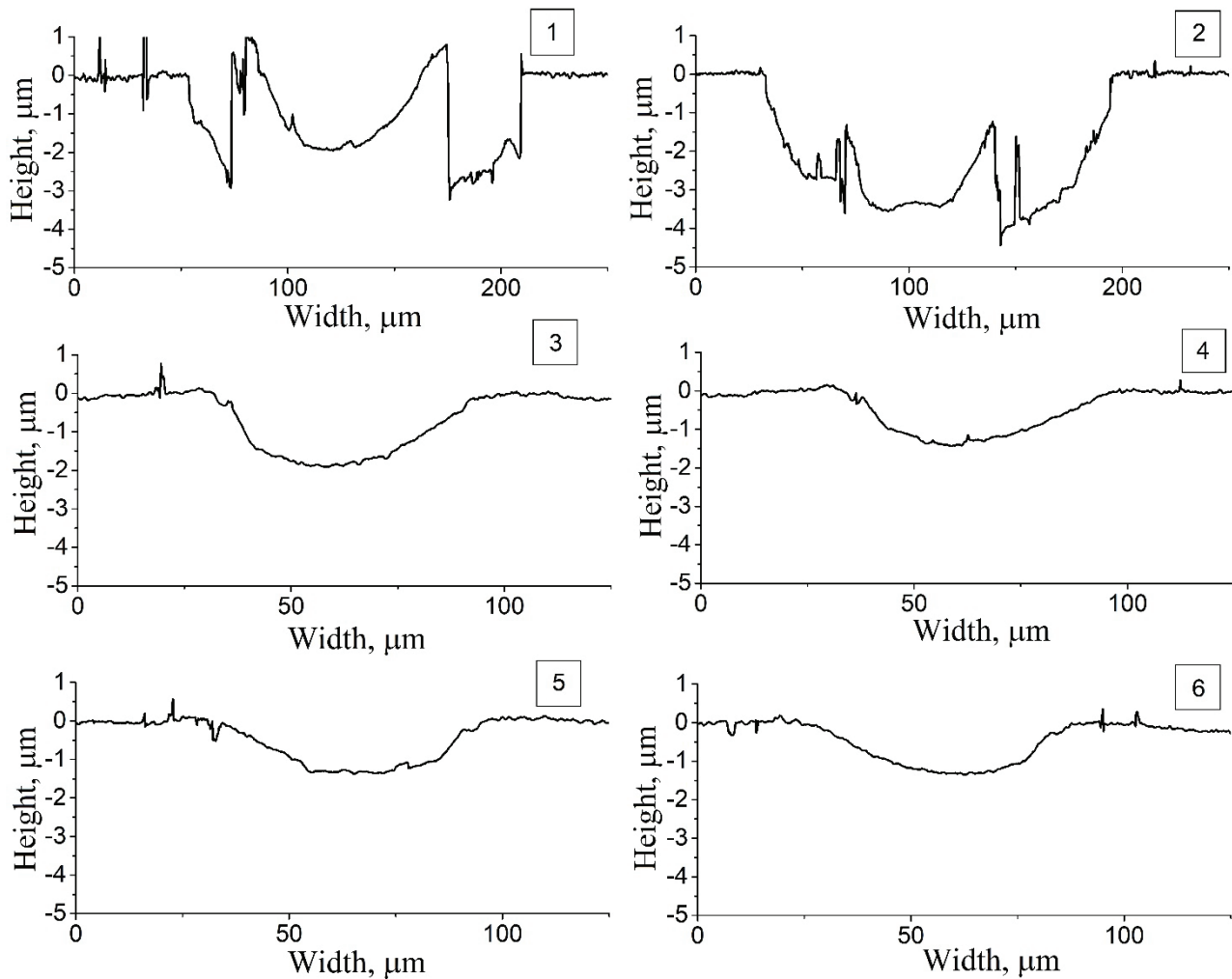


Fig. 9. Cross-sectional profiles of surface scratches on coatings: *CrN* (1), *ZrN* (2), *ZrCrN-1* (3), *ZrCrN-2* (4), *ZrCrN-3* (5), *ZrCrN-4* (6)

Table 2

Scratch profile parameters

Sample	Maximum scratch depth, µm	Maximum scratch depth along the cleavage, µm
<i>CrN</i>	3.52	4.50
<i>ZrN</i>	2.00	3.30
<i>ZrCrN-1</i>	1.88	–
<i>ZrCrN-2</i>	1.42	–
<i>ZrCrN-3</i>	1.32	–
<i>ZrCrN-4</i>	1.31	–

morphology of the coatings. This agrees with the surface roughness measurement results. A more pronounced surface roughness of *ZrCrN* coatings (Fig. 2) leads to large indentation depth fluctuations compared with smoother *CrN* and *ZrN* coatings. One can also see from Fig. 10 that the indentation depth sharply increases in *CrN* and *ZrN* coatings after ~2.3 mm of the scratch length, indicating significant damage to these coatings.

The data obtained show that the nanohardness measurement results (Table 1) are consistent with the scratch test results (Table 2). The hardest coatings are less susceptible to scratch damage. Note that none of the presented *ZrCrN* coatings showed signs of complete detachment, which implies its good adhesion to the substrate material.

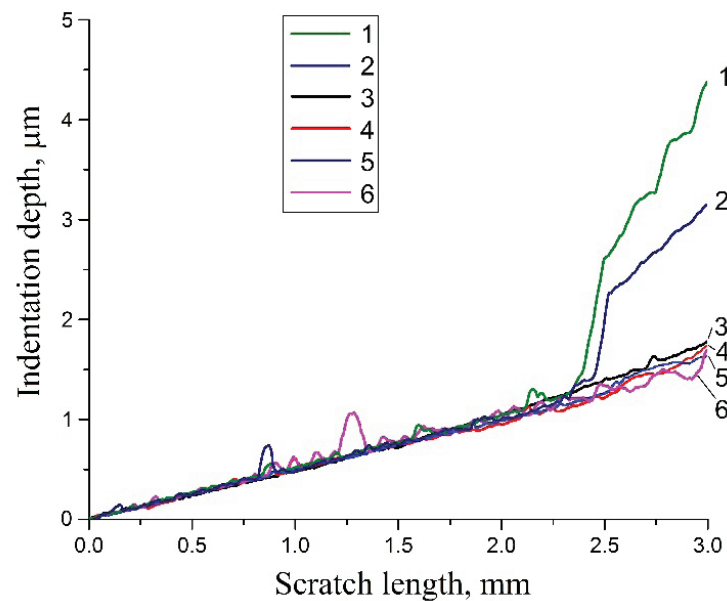


Fig. 10. Indentation depth variation profiles during scratching coatings: *CrN* (1), *ZrN* (2), *ZrCrN-1* (3), *ZrCrN-2* (4), *ZrCrN-3* (5), *ZrCrN-4* (6).

CrN coating, judging from the greatest scratch depth along the cleavage (Table 2), locally detached from the substrate during fracture, which can be explained by its high brittleness against diamond indentation. *ZrN* coating, judging from the same value (Table 2), was not damaged over the entire thickness, as it has higher mechanical properties compared to *CrN*. The review of literature in [19] provides similar information on the fracture of *ZrN*, *CrN*, and *CrN/ZrN* coatings, showing that multilayer *CrN/ZrN* coatings have better properties compared to *ZrN* and *CrN* coatings.

Conclusions

Experimental studies were performed to investigate the structure, phase composition, and mechanical properties of *CrN*, *ZrN*, and *ZrCrN* coatings. It was found that the structure, morphology, surface roughness, and mechanical properties of multilayer *ZrCrN* coatings are greatly affected by changes in the deposition conditions.

X-ray diffraction analysis data indicate the absence of pronounced texture in *ZrCrN-2...ZrCrN-4* coatings, and the broadening of the reflections is testimony to the nanostructured state of the layers. An increase in the rotation speed of the substrate holder relative to the *Cr* and *Zr* cathodes leads to a more pronounced surface microroughness. Increasing the holder rotation speed from 0.5 to 8 rpm during coating deposition causes an ~38 % monotonic increase in surface roughness in terms of the *Sa* parameter. The change in terms of the *Sz* parameter is less significant and does not exceed 12 %.

The investigation results showed that by varying the deposition conditions it is possible to obtain a *ZrCrN* coating (*ZrCrN-4* sample) with a high nanohardness of 45 GPa on *VK8* alloy. The nanohardness of multilayer *ZrCrN* coatings is by a factor of 1.14–2.1 higher than that of *CrN* and *ZrN* coatings. The *H/E* ratio values indicate that *ZrCrN-2...ZrCrN-4* coatings are more resistant to mechanical loads.

Scratch tests revealed that fracture of *CrN* and *ZrN* coatings occurs by the cohesive mechanism. The surface of multilayer *ZrCrN* coatings exhibits uniform scratches without signs of coating fracture. The results obtained confirmed good adhesion of all the studied coatings to the substrate.

Based on the study results, *ZrCrN-2...ZrCrN-4* coatings can be recommended for use as hard and wear-resistant coatings.

The results obtained will be used for more detailed XRD studies of multilayer coatings using synchrotron radiation from the VEPP-3 storage ring of the Siberian Synchrotron Radiation Center at the Budker Institute of Nuclear Physics SB RAS.



References

1. Khadem M., Penkov O.V., Yang H.K., Kim D.E. Tribology of multilayer coatings for wear reduction: a review. *Friction*, 2017, vol. 5 (3), pp. 248–262. DOI: 10.1007/s40544-017-0181-7.
2. Krella A. Resistance of PVD coatings to erosive and wear processes: a review. *Coatings*, 2020, vol. 10 (10), p. 921. DOI: 10.3390/COATINGS10100921.
3. Kameneva A.L., Sushentsov N.I., Klochkov A. Zavisimost' morfologii, svoistv, teplovogo i napryazhennogo sostoyaniya plenok ot tekhnologicheskikh parametrov magnetronnogo raspyleniya [Dependence of morphology, properties, thermal and stressed states of films on process parameters of electric arc evaporation]. *Tekhnologiya metallov = Metall Technology*, 2010, no. 11, pp. 38–42. (In Russian).
4. Pogrebnyak A.D., Shpak A.P., Beresnev V.M., Kolesnikov D.A., Kunitskii Yu.A., Sobol O.V., Uglov V.V., Komarov F.F., Shpylenko A.P., Makhmudov N.A., Demyanenko A.A., Baidak V.S., Grudnitskii V.V. Effect of thermal annealing in vacuum and in air on nanograin sizes in hard and superhard coatings Zr-Ti-Si-N. *Journal of Nanoscience and Nanotechnology*, 2012, vol. 12, no. 12, pp. 9213–9219. DOI: 10.1166/jnn.2012.6777.
5. Wu Z.T., Qi Z.B., Zhang D.F., Wang Z.C. Nanoindentation induced plastic deformation in nanocrystalline ZrN coating. *Materials Letters*, 2016, vol. 164, pp. 120–123. DOI: 10.1016/j.matlet.2015.10.091.
6. Gruss K.A., Zheleva T., Davis R.F., Watkins T.R. Characterization of zirconium nitride coatings deposited by cathodic arc sputtering. *Surface and Coatings Technology*, 1998, vol. 107, iss. 2–3, pp. 115–124. DOI: 10.1016/S0257-8972(98)00584-2.
7. Atar E., Çimenoglu H., Kayali E.S. Effect of oxidation on the wear behavior of a ZrN coating. *Key Engineering Materials*, 2005, vol. 280, pp. 1459–1462. DOI: 10.4028/www.scientific.net/kem.280-283.1459.
8. Musil J., Zenkin S., Kos Š., Čerstvý R., Haviar S. Flexible hydrophobic ZrN nitride films. *Vacuum*, 2016, vol. 131, pp. 34–38. DOI: 10.1016/j.vacuum.2016.05.020.
9. Mo J.L., Zhu M.H. Tribological characterization of chromium nitride coating deposited by filtered cathodic vacuum arc. *Applied Surface Science*, 2009, vol. 255, iss. 17, pp. 7627–7634. DOI: 10.1016/j.apsusc.2009.04.040.
10. Murakami R.I., Kim Y.H., Kimura K., Yonekura D., Shin D.H. Evaluation of adhesive behaviors of chromium nitride coating films produced by arc ion plating method. *JSME International Journal Series A, Solid Mechanics and Material Engineering*, 2006, vol. 49, iss. 1, pp. 123–129. DOI: 10.1299/jsmea.49.123.
11. Jagielski J., Khanna A.S., Kucinski J., Mishra D.S., Racolta P., Sioshansi P., Tobin E., Thereska J., Uglov V., Vilaithong T., Viviente J., Yang S.-Z., Zalar A. Effect of chromium nitride coating on the corrosion and wear resistance of stainless steel. *Applied Surface Science*, 2000, vol. 156, iss. 1–4, pp. 47–64. DOI: 10.1016/S0169-4332(99)00350-5.
12. Park J., Kusumah P., Kim Y., Kim K., Kwon K., Lee C.K. Corrosion prevention of chromium nitride coating with an application to bipolar plate materials. *Electrochemistry*, 2014, vol. 82, iss. 8, pp. 658–662. DOI: 10.5796/electrochemistry.82.658.
13. Lousa A., Romero J., Martínez E., Esteve J., Montalà F., Carreras L. Multilayered chromium chromium nitride coatings for use in pressure die-casting. *Surface and Coatings Technology*, 2001, vol. 146, pp. 268–273. DOI: 10.1016/S0257-8972(01)01476-1.
14. Zhang Z.G., Rapaud O., Bonasso N., Mercs D., Dong C., Coddet C. Control of microstructures and properties of dc magnetron sputtering deposited chromium nitride films. *Vacuum*, 2008, vol. 82, iss. 5, pp. 501–509. DOI: 10.1016/j.vacuum.2007.08.009.
15. Wicinski P., Smolik J., Garbacz H., Kurzydłowski K.J. Thermal stability and corrosion resistance of Cr/CrN multilayer coatings on Ti6Al4V alloy. *Solid State Phenomena*, 2015, vol. 237, pp. 47–53. DOI: 10.4028/www.scientific.net/SSP.237.47.
16. Dasgupta A., Premkumar A., Lawrence F., Houben L., Kuppasami P., Luysberg M., Nagaraja K.S., Raghunathan V.S. Microstructure of thick chromium-nitride coating synthesized using plasma assisted MOCVD technique. *Surface and Coatings Technology*, 2006, vol. 201, iss. 3–4, pp. 1401–1408. DOI: 10.1016/j.surfcoat.2006.02.005.
17. Shapovalov Y.A., Lee D.B. High temperature oxidation of Ti Al (La) N coating deposited on a steel substrate by arc-ion plating. *Materials Science Forum*, 2006, vol. 510, pp. 410–413.
18. Milošev I., Strehblow H.H., Navinšek B. Comparison of TiN, ZrN and CrN hard nitride coatings: electrochemical and thermal oxidation. *Thin Solid Films*, 1997, vol. 303, iss. 1–2, pp. 246–254. DOI: 10.1016/S0040-6090(97)00069-2.



19. Maksakova O.V., Pogrebnjak O.D., Beresnev V.M. Features of investigations of multilayer nitride coatings based on Cr and Zr. *Uspekhi fiziki metallov = Progress in Physics of Metals*, 2018, vol. 19, no. 1. DOI: 10.15407/ufm.19.01.025.
20. Zhang Z.G., Rapaud O., Allain N., Merce D., Baraket M., Dong C., Coddet C. Microstructures and tribological properties of CrN/ZrN nanoscale multilayer coatings. *Applied Surface Science*, 2009, vol. 255, iss. 7, pp. 4020–4026. DOI: 10.1016/j.apsusc.2008.10.075.
21. Sánchez N.A. de, Jaramillo Suárez H.E., Vivas Z., Aperador W., Amaya C., Caicedo J.C. Fracture resistant and wear corrosion performance of CrN/ZrN bilayers deposited onto AISI 420 stainless steel. *Advanced Materials Research*, 2008, vol. 38, pp. 63–75. DOI: 10.4028/www.scientific.net/amr.38.63.
22. Kim M.K., Kim G.S., Lee S.Y. Synthesis and characterization of multilayer CrN/ZrN coatings. *Metals and Materials International*, 2008, vol. 14, no. 4, pp. 465–470. DOI: 10.3365/met.mat.2008.08.465.
23. Zhang J.J., Wang M.X., Yang J., Liu Q.X., Li D.J. Enhancing mechanical and tribological performance of multilayered CrN/ZrN coatings. *Surface and Coatings Technology*, 2007, vol. 201, iss. 9–11, pp. 5186–5189. DOI: 10.1016/j.surfcoat.2006.07.093.
24. Li D.J., Liu F., Wang M.X., Zhang J.J., Liu Q.X. Structural and mechanical properties of multilayered gradient CrN/ZrN coatings. *Thin Solid Films*, 2006, vol. 506, pp. 202–206. DOI: 10.1016/j.tsf.2005.08.031.
25. Wang M.X., Zhang J.J., Liu Q.X., Li D.J. Magnetron sputtering deposition of polycrystalline CrN/ZrN superlattice coatings. *Surface Review and Letters*, 2006, vol. 13, no. 2–3, pp. 173–177. DOI: 10.1142/s0218625x06008177.
26. Sobol' O.V., Melekhov A.A., Postelnyk A.A., Andreev A.A., Stolbovoy V.A., Gorban' V.F. Vozmozhnosti strukturnoi inzhenerii v mnogosloynnykh vakuumno-dugovykh ZrN/CrN-pokrytyakh putem izmeneniya tolshchiny nanosloev i podachi potentsiala smeshcheniya [Possibilities of structural engineering in multilayer vacuum-arc ZrN/CRN coatings by varying the nanolayer thickness and application of a bias potential]. *Zhurnal tekhnicheskoi fiziki = Technical Physics*, 2016, vol. 86, no. 7, pp. 100–103. (In Russian).
27. Sobol' O.V., Andreev A.A., Gorban' V.F., Stolbovoy V.A., Melekhov A.A., Postelnyk A.A., Dolomanov A.V. Influence of pressure of working atmosphere on the formation of phase-structural state and physical and mechanical properties of vacuum-arc multilayer coatings ZrN/CrN. *Voprosy atomnoi nauki i tekhniki = Problems of Atomic Science and Technology*, 2016, no. 1 (101), pp. 134–139.
28. Sobol' O.V., Andreev A.A., Gorban' V.F., Melekhov A.A., Postelnyk A.A., Stolbovoy V.A. Structural engineering of the vacuum Arc ZrN/CrN multilayer coatings. *Journal of Nano- and Electronic Physics*, 2016, vol. 8, no. 1, p. 01042-1.
29. Chen S.F., Kuo Y.C., Wang C.J., Huang S.H., Lee J.W., Chan Y.C., Duh J.G., Hsieh T.E. The effect of Cr/Zr chemical composition ratios on the mechanical properties of CrN/ZrN multilayered coatings deposited by cathodic arc deposition system. *Surface and Coatings Technology*, 2013, vol. 231, pp. 247–252. DOI: 10.1016/j.surfcoat.2012.03.002.
30. Huang S.H., Chen S.F., Kuo Y.C., Wang C.J., Lee J.W., Chan Y.C., Chen H.W., Duh J.G., Hsieh T.E. Mechanical and tribological properties evaluation of cathodic arc deposited CrN/ZrN multilayer coatings. *Surface and Coatings Technology*, 2011, vol. 206, iss. 7, pp. 1744–1752. DOI: 10.1016/j.surfcoat.2011.10.029.
31. Samim P.M., Fattah-alhosseini A., Elmkhah H., Imantalab O. Nanoscale architecture of ZrN/CrN coatings: microstructure, composition, mechanical properties and electrochemical behavior. *Journal of Materials Research and Technology*, 2021, vol. 15, pp. 542–560. DOI: 10.1016/j.jmrt.2021.08.018.
32. Tarasov S.Yu., Filippov A.V., Savchenko N.L., Fortuna S.V., Rubtsov V.E., Kolubaev E.A., Psakhie S.G. Effect of heat input on phase content, crystalline lattice parameter, and residual strain in wire-feed electron beam additive manufactured 304 stainless steel. *International Journal of Advanced Manufacturing Technology*, 2018, vol. 99, pp. 2353–2363. DOI: 10.1007/s00170-018-2643-0.

Conflicts of Interest

The authors declare no conflict of interest.

© 2022 The Authors. Published by Novosibirsk State Technical University. This is an open access article under the CC BY license (<http://creativecommons.org/licenses/by/4.0/>).